DNAX-activating Protein 10 (DAP10) Membrane Adaptor Associates with Receptor for Advanced Glycation End Products (RAGE) and Modulates the RAGE-triggered Signaling Pathway in Human Keratinocytes[*]

Masakiyo Sakaguchi[‡1], Hitoshi Murata[‡], Yumi Aoyama[§], Toshihiko Hibino[¶], Endy Widya Putranto[‡],
I. Made Winarsa Ruma[‡], Yusuke Inoue[∥], Yoshihiko Sakaguchi[**], Ken-ichi Yamamoto[‡], Rie Kinoshita[‡‡],
Junichiro Futami[‡‡], Ken Kataoka[§§], Keiji Iwatsuki[§], and Nam-ho Huh[‡]

From the Departments of [‡]Cell Biology and [§]Dermatology, Okayama University Graduate School of Medicine, Dentistry and Pharmaceutical Sciences, 2-5-1 Shikatacho, Kita-ku, Okayama 700-8558, the [¶]Shiseido Research Center, Advanced Science Research, 2-2-1 Hayabuchi, Tsuzuki-ku, Yokohama 224-8558, the [∥]Faculty of Science and Technology, Division of Molecular Science, Gunma University, 1-5-1 Tenjin-cho, Kiryu, Gunma 376-8515, the [**]Interdisciplinary Research Organization, University of Miyazaki, Kiyotakecho, Miyazaki 889-1692, the [‡‡]Department of Biotechnology, Division of Chemistry and Biochemistry, Graduate School of Natural Science and Technology, Okayama University, Okayama 700-8530, and the [§§]Department of Life Science, Faculty of Science, Okayama University of Science, 1-1 Ridai-cho, Kita-ku, Okayama 700-0005, Japan

Background: RAGE receptor plays a critical role in many inflammatory disorders.
Results: Functional interaction between RAGE and DAP10 coordinately regulates S100A8/A9-mediated cell survival.
Conclusion: DAP10 membrane adaptor is critically involved in RAGE-mediated survival signaling upon S100A8/A9 binding.
Significance: This is the first report demonstrating that RAGE-mediated survival signaling is critically regulated by DAP10 interaction.

The receptor for advanced glycation end products (RAGE) is involved in the pathogenesis of many inflammatory, degenerative, and hyperproliferative diseases, including cancer. Previously, we revealed mechanisms of downstream signaling from ligand-activated RAGE, which recruits TIRAP/MyD88. Here, we showed that DNAX-activating protein 10 (DAP10), a transmembrane adaptor protein, also binds to RAGE. By artificial oligomerization of RAGE alone or RAGE-DAP10, we found that RAGE-DAP10 heterodimer formation resulted in a marked enhancement of Akt activation, whereas homomultimeric interaction of RAGE led to activation of caspase 8. Normal human epidermal keratinocytes exposed to S100A8/A9, a ligand for RAGE, at a nanomolar concentration mimicked the pro-survival response of RAGE-DAP10 interaction, although at a micromolar concentration, the cells mimicked the pro-apoptotic response of RAGE-RAGE. In transformed epithelial cell lines, A431 and HaCaT, in which endogenous DAP10 was overexpressed, and S100A8/A9, even at a micromolar concentration, led to cell growth and survival due to RAGE-DAP10 interaction. Functional blocking of DAP10 in the cell lines abrogated the Akt phosphorylation from S100A8/A9-activated RAGE, eventually leading to an increase in apoptosis. Finally, S100A8/A9, RAGE, and DAP10 were overexpressed in the psoriatic epidermis. Our findings indicate that the functional interaction between RAGE and DAP10 coordinately regulates S100A8/A9-mediated survival and/or apoptotic response of keratinocytes.

The receptor for advanced glycation end products (RAGE)[2] is involved in diverse physiological and pathological processes related to inflammation (1–5). RAGE binds to a wide variety of ligands, including advanced glycation end products, S100 proteins, amyloid β, and high mobility group box protein 1 (HMGB1) (6). Upon binding of ligands, RAGE triggers different intracellular signaling pathways (7, 8). One of the mechanisms for the complex signal processing involving RAGE is sharing of ligands by RAGE and other receptors. For example, advanced glycation end products also bind to galectin-3, fasciclin, EGF-like, laminin-type EGF-like, and link domain-containing scavenger receptor-1 (FEEL1), fasciclin, EGF-like, laminin-type EGF-like, and link domain-containing scavenger receptor-2 (FEEL2), cluster of differentiation 36 (CD36), scavenger receptor class A, scavenger receptor class B member 1, and lectin-type oxidized LDL receptor 1 (LOX-1) (9–14), whereas amyloid β and HMGB1 bind to Toll-like receptors (TLRs) (15, 16), and S100A8/A9 binds to Emmprin (17).

S100A8/A9, one of the 20 S100 proteins, plays a pivotal role in the skin through RAGE (5, 18). Zenz et al. (19) showed that induction of S100A8/A9 is one of the earliest events in the

[2] The abbreviations used are: RAGE, receptor for advanced glycation end product; TLR, Toll-like receptor; NHK, normal human keratinocyte; TRIF, TIR-domain-containing adaptor-inducing interferon-β; NF-κB, nuclear factor κ-light-chain enhancer of activated B cell; IP, immunoprecipitation; SH2, Src homology 2; TIRAP, Toll-interleukin 1 receptor domain-containing adaptor protein.

pathogenesis of psoriasis in a mouse model. In addition, serum S100A8/A9 was increased in patients with psoriasis vulgaris and general pustular psoriasis (20), and S100A8/A9 was shown to stimulate the growth of normal human keratinocytes (NHKs) (18).

An additional mechanism is interference among receptors and adaptor proteins. We recently found that, upon ligand binding, RAGE recruits TIRAP and MyD88, well known adaptor proteins for TLR2 and -4, for downstream signal transduction (21). At the same time, RAGE and TLR4 have unique adaptor proteins, diaphanous 1 and TRIF-related adaptor molecule/TRIF, respectively (22, 23).

Zong *et al.* (24) reported that homodimerization of RAGE is essential for RAGE-mediated signal transduction, leading to activations of p44/p42 MAPK (ERK1/2) and NF-κB in HEK293T cells. Moreover, Slowik *et al.* (25) showed that formyl peptide receptors, to which amyloid-β can bind, interact with RAGE and augment the enhanced signal transduction of ERK1/2 in HEK293 cells. However, Emmprin and TLR2/4 do not directly interact with RAGE.[3]

In this study, we tried to identify possible receptors and transmembrane adaptor proteins that interact with RAGE, with a focus on immune response and inflammation. We found that DNAX-activating protein 10 (DAP10), a transmembrane adaptor protein for natural killer group 2, member D (NKG2D), directly binds to RAGE and modulates the S100A8/A9-triggered signaling pathway. DAP10 as well as S100A8/A9 and RAGE were overexpressed in psoriatic epidermis.

EXPERIMENTAL PROCEDURES

Reagents—The following reagents were purchased from commercial sources: B/B homodimerizer and A/C heterodimerizer, Clontech; Akt inhibitor, Calbiochem-EMD Millipore; recombinant human TGF-β, Sigma; recombinant human EGF, TNF-α, and IL-17, PeproTech EC (London, UK); recombinant human IL-22, R&D Systems (Minneapolis, MN); tritiated thymidine, ARC (St. Louis, MO); and FITC-labeled annexin V, MBL (Nagoya, Japan).

Cell Culture—Neonatal normal human epidermal keratinocytes (KURABO, Osaka, Japan) were cultured in serum-free 154S medium (KURABO) containing HKGS growth supplement (KURABO) and used for experiments between passages 2 and 4. HaCaT, a gift from Dr. Fusenig (German Cancer Research Center, Heidelberg, Germany), A431 (ATCC, Rockville, MD), and HEK293T (RIKEN Bio Resource Center, Tsukuba, Japan) were cultured in D/F medium (Invitrogen) supplemented with 10% fetal bovine serum (FBS; Intergen, Purchase, NY). For quantitation of apoptosis, the fluorescence intensity of annexin V-labeled cells was determined using a fluorescence microplate reader (Fluoroskan Ascent FL; Thermo Fisher Scientific Inc., Waltham, MA). For cross-linking of endogenous RAGE, BS3 (Sulfo-DSS; Thermo Scientific) was applied to cells according to the protocol reported previously (24).

Vector Constructs for Expression in Mammalian Cells—cDNAs were inserted into the pIDT-CMVi vector (21). A total of seven fragments (SP-V-C1-C2-TM, SP-V-TM, SP-C1-TM, SP-C2-TM, SP-V-C1-TM, SP-C1-C2-TM, and SP-V-C1-C2) from the full-length RAGE (SP-V-C1-C2-TM-cyt) was constructed for expression as C-terminal (Myc-HA-FLAG-His$_6$)-tagged forms. (SP indicates signal peptide sequence (1–22 amino acids); V indicates variable (V)-type immunoglobulin domain (23–132 amino acids); C1 indicates constant (C)-type immunoglobulin domain 1 (133–243 amino acids); C2 indicates C-type immunoglobulin domain 2 (244–342 amino acids); TM indicates hydrophobic transmembrane-spanning domain (343–363 amino acids); and cyt indicates short cytoplasmic domain (364–404 amino acids).) Human cDNAs encoding full-length TLR4, TNFR1, TNFR2, DAP10/HCST (DAP10; WT and mut Y86F), γc/common γ-chain/IL2RG/CD132 (γc), and gp130/IL6ST/CD130 (gp130) were designed for expression as C-terminal 3×FLAG-His$_6$-tagged forms. Nine kinds of Src homology 2 (SH2) domain-containing adaptor proteins (PI3K-p85, growth factor receptor-bound protein 2) (GRB2), growth factor receptor-bound protein 7 (GRB7), NCK1, NCK2, CRK, SOCS, SHC, and SHP2) were tagged with C-terminal 3×Myc-His$_6$-tagged forms.

For regulated dimerization/polymerization, we used an iDimerize^{TM}-inducible expression system (Clontech TAKARA) that allows specific interaction by treatment with dimerizers as follows: 1) transfection with DmrB-DmrB-RAGE-cyt (364–404 amino acids)-3×HA-His$_6$ followed by B/B homodimerizer treatment for homopolymerization of RAGE; 2) transfection with DmrA-DmrB-RAGE-cyt-3×HA-His$_6$, and DmrC-DmrB-RAGE-cyt-3×FLAG-His$_6$ followed by A/C heterodimerizer treatment for RAGE homodimerization; and 3) transfection with DmrA-DmrB-RAGE-cyt-3×HA-His$_6$ and DmrC-DmrB-DAP10-cyt (70–93 amino acids)-3×FLAG-His$_6$ followed by A/C heterodimerizer treatment for RAGE-DAP10 heterodimerization. The proteins have a myristylation signal at the N-terminal site. FuGENE-HD (Promega BioSciences, San Luis Obispo, CA) was used for transfection.

Preparation of S100A8/A9 Proteins—Human S100A8 and S100A9 cDNAs were cloned into the pGEX-6P1 vector (GE Healthcare) for expression in *Escherichia coli*. Purification and heterodimerization of S100A8/A9 were performed under conditions reported previously (17, 18, 21). The amounts of contaminating endotoxins (LPS and β-glucans) were 0.008 EU/mg for S100A8/A9 and 0.013 EU/mg for GST as determined with a *Limulus* amebocyte lysate assay (Seikagaku Corp., Tokyo, Japan).

Western Blot (WB) Analysis and Immunoprecipitation (IP)—WB analysis was performed under conventional conditions. The following antibodies were used for Western blot analysis: mouse anti-human DAP10, mouse anti-human RAGE (A-9), and rabbit anti-human PKCζ antibodies (Santa Cruz Biotechnology, Santa Cruz, CA); rabbit anti-human phospho-PKCζ-(Thr-560) antibody (Epitomics Abcam, Burlingame, CA); mouse anti-HA tag (clone 6E2), mouse anti-Myc tag (clone 9B11), rabbit anti-human p38, rabbit anti-human phospho-p38 (Thr-180/Tyr-182), rabbit anti-human Akt, rabbit anti-human phospho-Akt (Ser-473), rabbit anti-human phospho-Akt

(Thr308), rabbit anti-human NF-κB(p65), rabbit anti-human phospho-NFKB(p65) (Ser-536), mouse anti-human cleaved caspase 8 (Asp-384), and mouse anti-phosphotyrosine (Tyr(P)-102) antibodies (Cell Signaling Technology, Beverly, MA); rabbit anti-human TIRAP antibody (Abcam, Cambridge, UK); rabbit anti-human MyD88 and mouse anti-human PI3K (p85) antibodies (MBL, Nagoya, Japan); and mouse anti-FLAG tag (clone M2) and mouse anti-human tubulin antibodies (Sigma). Rabbit anti-human phospho-RAGE (Ser-391) antibody was obtained by ordering from a custom antibody production service at MBL (the immunized phosphopeptide was AELNQS-(phospho)EEPEC).

For immunohistochemical analysis, the following antibodies were used: mouse anti-human calprotectin antibody (S100A8/A9 heterodimer) (Hycult Biotech, Plymouth Meeting, PA); mouse anti-human RAGE (A-9) antibody (Santa Cruz Biotechnology); mouse anti-human DAP10 antibody (Santa Cruz Biotechnology); and rabbit anti-human phospho-Akt (Ser-473) antibody (Epitomics Abcam).

For pulldown analysis of endogenous RAGE, rabbit anti-human RAGE (H-300) antibody (Santa Cruz Biotechnology) was biotinylated using a Biotin labeling kit-SH (Dojindo Molecular Technologies, Rockville, MD) to recover antibody-free RAGE after IP using streptavidin-agarose (21). The second antibody was horseradish peroxidase-conjugated anti-mouse or anti-rabbit IgG antibody (Cell Signaling Technology). Positive signals were detected by a chemiluminescence system (ECL Plus; GE Healthcare).

Monoclonal anti-HA (clone HA-7) tag-agarose (Sigma), monoclonal anti-Myc tag (clone 1G4)-agarose (MBL), and streptavidin-agarose (Invitrogen) were used for co-IP experiments. The levels of the GTP-bound forms of Rac1 and Cdc42 were determined by using a Rac/Cdc42 activation assay kit (Millipore).

Immunohistochemistry—Human skin samples were obtained after receiving written informed consent under conditions approved by the Research Ethics Committee of Okayama University Medical School Hospital, Japan. Paraffin sections were subjected to autoclaving (121 °C for 20 min) in sodium citrate buffer, followed by treatment with L.A.B solution (Polysciences, Warrington, PA) at room temperature for 30 min. The sections were incubated first with antibodies, followed by treatment with highly cross-adsorbed Alexa Fluor 594-conjugated (for S100A8/A9 and RAGE) or Alexa Fluor 488 (for DAP10)-conjugated goat anti-mouse IgG antibodies and Alexa Fluor 594-conjugated goat anti-rabbit IgG antibody (for phospho-Akt) (Molecular Probes Invitrogen). SYBR Green I (Cambrex, Rockland, ME) was used for counterstaining of cell nuclei.

RNA Interference—Human DAP10/HCST (siDAP10, siGENOME SMART pool M-005100-02-0005), human RAGE/AGER (siRAGE, siGENOME SMART pool M-003625-02-0005), and negative control (siCont, siGENOME nontargeting siRNA pool 1, D-001210-01) siRNAs were purchased from Thermo Scientific Dharmacon (Lafayette, CO). The siRNAs (100 nM) were transfected using Lipofectamine RNAiMAX reagent (Invitrogen).

Statistical Analysis—Data are expressed as the means ± S.D. We employed a simple pairwise comparison using Student's t test (two-tailed distribution with a two-sample equal variance). Values of $p < 0.05$ were considered statistically significant.

RESULTS

DAP10 Associates with RAGE via Its Transmembrane Region—S100A8/A9, one of the 20 S100 proteins, plays a pivotal role in cutaneous inflammation with epidermal proliferation through RAGE binding (5, 18). In this study, we tried to identify possible RAGE interacting receptor/adaptor proteins that may facilitate this role by focusing on those related to immune response and inflammation. An authentic approach in which membrane proteins that co-precipitated with RAGE were analyzed by LC-MS/MS did not yield any promising candidates (data not shown). In addition, Emmprin, which shares the same ability to bind the S100A9 ligand (17), also did not show interaction with RAGE (data not shown). We therefore employed a candidate-based screening using inflammatory receptors (TLR4, TNFR1, and TNFR2) and membrane proteins (γc, gp130, and DAP10), which co-functioned with cytokine receptors. As shown in Fig. 1*A*, only DAP10, a transmembrane adaptor protein for NKG2D (26), was co-precipitated with RAGE among the proteins examined. Interaction of RAGE with DAP10 was confirmed in different experimental settings, using the already known binding between NKG2D and DAP10 as a positive control (Fig. 1*B*). We also excluded the possibility that DAP10 indirectly bound to RAGE via NKG2D because RAGE did not show interaction with NKG2D (Fig. 1*C*). To investigate the nature of binding between RAGE and DAP10, we used various deletion mutants of RAGE. Among the mutants, only a RAGE variant lacking the transmembrane region (V-C1-C2) failed in binding to DAP10 (Fig. 1*D*), indicating that both proteins interact through the transmembrane domain.

DAP10 in its interaction with NKG2D is known to recruit SH2 domain-containing adaptor molecules such as PI3K and GRB2 (27, 28). We therefore examined whether these recruitments could also occur downstream of the RAGE-DAP10 interaction, and indeed we found that PI3K and GRB2 were co-precipitated with RAGE-DAP10. In addition, we found that GBR7, another SH2-domain-containing adaptor protein, was also co-precipitated with RAGE-DAP10 (Fig. 1*E*). Furthermore, the recruitments of PI3K, GRB2, and GRB7 were all abrogated by replacement of Tyr-86 with nonphosphorylatable Phe in the cytoplasmic domain of DAP10 (Y86F) (Fig. 1*F*), as reported previously (27). These results indicate that DAP10 may function as a transmembrane adaptor protein for RAGE (Fig. 1*G*).

Modulation of RAGE-triggered Signaling by DAP10—To gain insight into the effect of DAP10 on RAGE signaling, we used an artificial oligomerization system that enabled us to specifically form RAGE-DAP10 heterodimers and also RAGE homomultimers and homodimers for comparisons (Fig. 2, *A* and *B*, *top panel*). In accordance with the results of our previous study (21), multimerization and dimerization of RAGE alone resulted in recruitment of PKCζ, TIRAP, and MyD88 with phosphorylation of PKCζ (Thr-560) and RAGE (Ser-391) in HEK293 cells. PI3K, which linked to the activation of Akt, was recruited at a remarkable level to the heterodimer of RAGE and DAP10 (RAGE-DAP10) and also at a lower level to the RAGE homodimers $(RAGE)_2$ and homomultimers $(RAGE)_M$ (Fig. 2*B*).
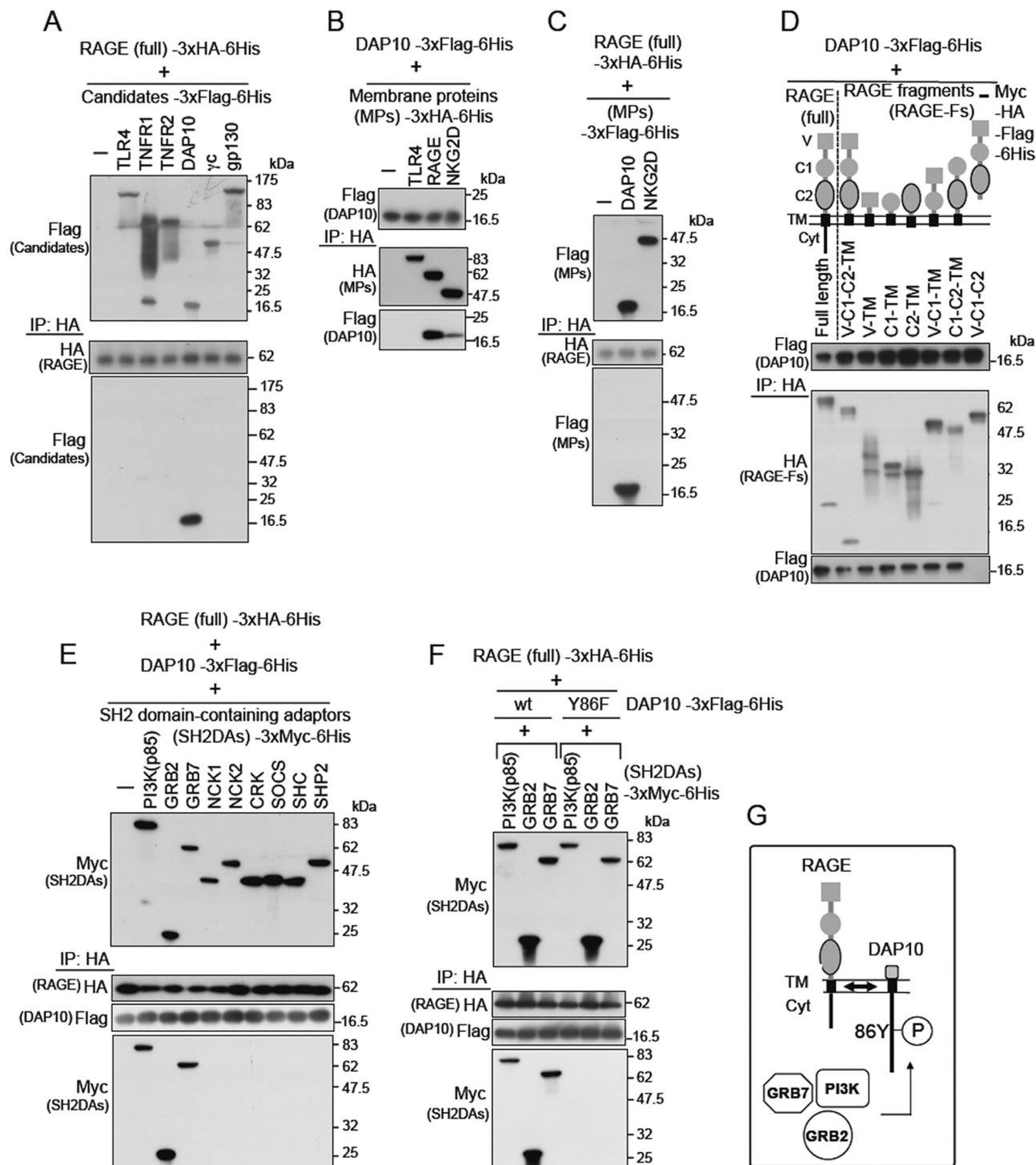
FIGURE 1. **Association of DAP10 with RAGE.** *A,* screening for receptors interacting with RAGE. HEK293T cells were co-transfected with RAGE (*full*, full-length)-3×HA-His$_6$ and candidates (TLR4, TNFR1, TNFR2, DAP10, γc, and gp130) tagged with 3×HA-His$_6$. Twenty four hours after transfection, cell extracts were prepared and analyzed by Western blotting both with and without prior IP using anti-HA tag beads for the expressed RAGE. *B,* confirmation analysis of the RAGE-DAP10 interaction including a positive binding control, NKG2D-DAP10. A co-transfection experiment was performed as described in *A* using the combinations: DAP10–3×FLAG-His$_6$ with membrane proteins (*MP*: TLR4, RAGE, and NKG2D) tagged with 3×HA-His$_6$. *C,* NKG2D-independent binding of DAP10 to RAGE. Co-transfection and IP analysis were performed as in *A* and *B* using the combinations of RAGE (*full*)-3×HA-His$_6$ with membrane proteins (DAP10 and NKG2D) tagged with 3×FLAG-His6. *D,* identification of an indispensable region of RAGE for association with DAP10. Full-length (*full*) RAGE and its seven fragments (*RAGE-Fs*) tagged with Myc-HA-FLAG-His$_6$ were co-transfected with DAP10–3×FLAG-His$_6$ into HEK293T cells. Preparation of cell extracts and the subsequent IP experiments was performed under conditions similar to those in *A, B,* and *C. E,* identification of downstream adaptors for DAP10-RAGE. Simultaneous transfections of RAGE (*full*)-3×HA-His$_6$ and DAP10–3×FLAG-His$_6$ with SH2 domain-containing adaptors (*SH2DAs*: PI3K-p85, GRB2, GRB7, NCK1, NCK2, CRK, SOCS, SHC, and SHP2) tagged with 3×Myc-His$_6$ were performed. Twenty four hours after transfection, cell extracts were prepared and analyzed by Western blotting both with and without prior IP using anti-HA tag beads for the expressed RAGE. *F,* DAP10-dependent interaction of the adaptors (PI3K-p85, GRB2, and GRB7) with the RAGE-DAP10 receptor complex. Simultaneous transfection of RAGE (*full*)-3×HA-His$_6$, DAP10–3×FLAG-His$_6$, and one of the SH2DAs (PI3K-p85, GRB2, and GRB7)-3×HA-His$_6$ followed by IP was performed under conditions similar to those in *E* with the inclusion of a nonphosphorylatable DAP10 (Y86F is tyrosine 86 replaced with phenylalanine). Y86F abrogates recruitment of the downstream adaptor proteins. *G,* schematic illustration of the interaction among RAGE, DAP10, and adaptor proteins.
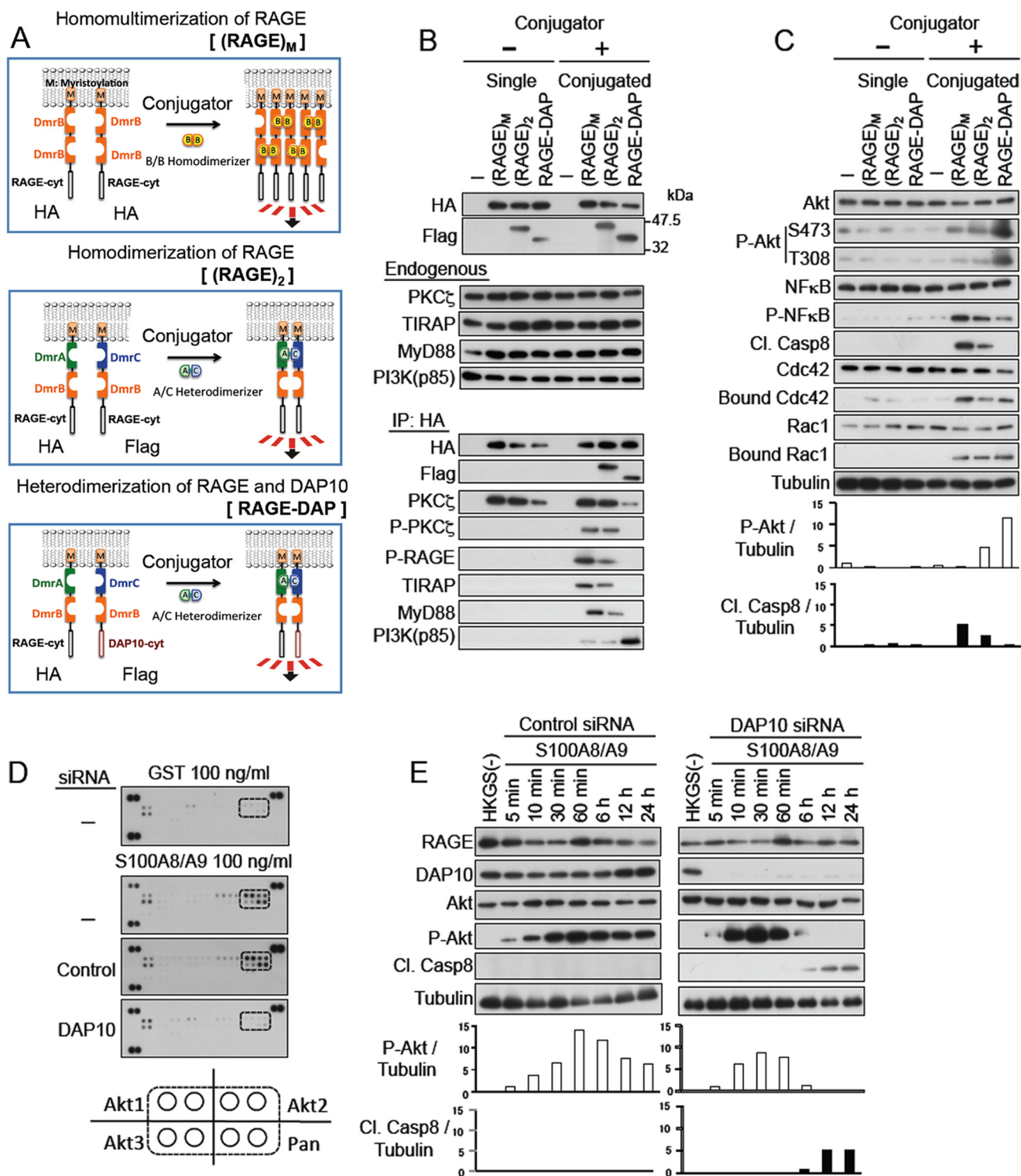
FIGURE 2. **RAGE differential signal transduction with or without the presence of DAP10 association.** *A,* schematic presentation of the procedure for homomultimerization ((*RAGE*)$_M$) (*top*) and homodimerization ((*RAGE*)$_2$) (*middle*) of RAGE-cyt and heterodimerization (*RAGE-DAP*) of RAGE-cyt and DAP10-cyt (*bottom*). *B,* recruitment of differential adaptor proteins with or without involvement of DAP10. HEK293T cells were transfected with DmrB-DmrB-RAGE-cyt-3×HA-His$_6$ alone ((*A*) *top*), DmrA-DmrB-RAGE-cyt-3×HA-His$_6$, and DmrC-DmrB-RAGE-cyt-3×FLAG-His$_6$ ((*A*) *middle*), or DmrA-DmrB-RAGE-cyt-3×HA-His$_6$ and DmrC-DmrB-DAP10-cyt-3×FLAG-His$_6$ ((*A*) *bottom*). Twenty four hours after transfection, the cells were then treated or not treated with conjugators (50 nM, 1 h) (B/B homodimerizer or A/C heterodimerizer) and subjected to Western blot analysis both with and without prior IP using anti-HA tag beads for the expressed DmrB-DmrB-RAGE-cyt or DmrA-DmrB-RAGE-cyt. *P-,* phosphorylated. *C,* differential activation of downstream molecules with or without involvement of DAP10 examined as in *B*. Ser-473 and Thr-308, phosphorylated Akt at the residues; *Cl. Casp8,* cleaved caspase 8; *Bound,* activated form. *Bar graphs,* quantified levels of phosphorylated Akt and cleaved caspase 8 relative to tubulin. ImageJ (rsb.info.nih.gov) was used to compare the band density of Western blots. *D,* screening for phosphorylated kinases in NHKs treated with the indicated siRNAs (100 nM, 48 h) and subsequent exposure to GST or S100A8/A9 (100 ng/ml, 24 h) using a phospho-MAPK array (R&D Systems). *E,* time course experiments for the effect of siRNAs on Akt activation induced by S100A8/A9 (100 ng/ml) in NHKs. *Bar graphs,* quantified levels of phosphorylated Akt and cleaved caspase 8 relative to tubulin.
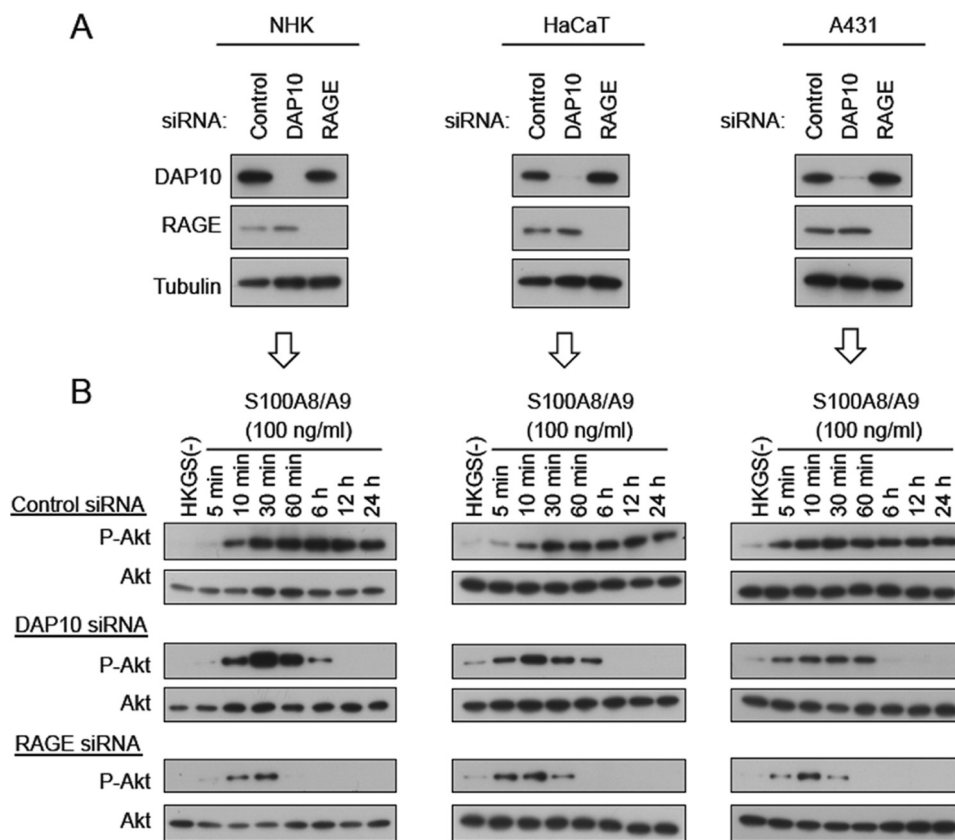
FIGURE 3. **Effects of siRNAs on S100A8/A9-mediated activation of Akt.** *A,* inhibitory effects of siRNAs against DAP10 and RAGE. Seventy two hours after transfection with a negative control siRNA (*control*), DAP10 siRNA, and RAGE siRNAs, each at 100 nM, the treated cells were harvested and examined by Western blot analysis. *B,* time course experiments for the effect of siRNAs on Akt activation induced by S100A8/A9 (100 ng/ml) in NHKs, HaCaT, and A451 cells. Forty eight hours after transfection with the indicated siRNAs (*Control, DAP10,* and *RAGE*) in NHKs, the cells were treated with S100A8/A9 (100 ng/ml) for the indicated periods.

Laird *et al.* (29) reported that MyD88 also recruited PI3K to some extent. This therefore may explain the occurrence of a lower recruitment level of PI3K to RAGE homodimers and homomultimers via MyD88. In a following experiment, notably the RAGE-DAP10 heterodimer caused strong activation of Akt, although the RAGE homodimer and multimer resulted in higher activations of caspase 8 and NF-κB. Cdc42 and Rac1 were activated under both conditions, but the levels did not show any appreciable difference for the comparisons of the three different oligomerization systems (Fig. 2*C*). These results indicate that the involvement of DAP10 leads to modulation of RAGE-triggered signal transduction.

To study the possible role(s) of the physiological interaction of RAGE and DAP10 in the activation of effector kinases, NHKs were exposed to 100 ng/ml S100A8/A9, a physiological ligand for RAGE. We found that Akt, especially Akt1 and Akt2, was markedly phosphorylated, as demonstrated using a phosphokinase array (Fig. 2*D*). When DAP10 was down-regulated with siRNA, activation of Akt by S100A8/A9 was completely abrogated after 24 h of incubation (Fig. 2*D*). To examine the time course more precisely, NHKs were exposed to 100 ng/ml S100A8/A9 and analyzed by Western blotting. Akt was persistently activated from 5 min to 24 h in NHKs. Additionally, when DAP10 was down-regulated with siRNA, activation of Akt was transient and nullified after 6 h (Fig. 2*E*). Similar results were obtained in the transformed human keratinocyte cell lines

HaCaT and A431, with down-regulation of DAP10 (Fig. 3, *A* and *B*), indicating that DAP10 is mainly involved in the persistence of Akt activation.

To avoid the possibility that Akt activation by S100A8/A9 might have been produced through other receptors besides RAGE, we also monitored the kinetics of S100A8/A9-mediated Akt phosphorylation in cells in which RAGE expression was silenced by siRNA. Similar to the effects of DAP10 siRNA treatment, the use of RAGE siRNA resulted in abrogation of the persistent activation of Akt. The abrogation by RAGE siRNA was observed earlier, starting from 60 min, than that induced by DAP10 siRNA, suggesting a more upstream role (Fig. 3, *A* and *B*). In addition, similar activation kinetics of Akt was observed in NHKs after exposure to another well established RAGE ligand, S100B (data not shown). These results clearly indicate that RAGE and DAP10 are essential for the persistence of Akt activation.

Differential Response of Normal and Transformed Human Keratinocytes to S100A8/A9—When exposed to a low concentration of S100A8/A9 (100 ng/ml), both NHKs and the transformed human keratinocyte cell lines, HaCaT and A431, exhibited a similar strong and persistent activation of Akt without activation of caspase 8 (Fig. 4*A*). Conversely, exposure to a high concentration of S100A8/A9 (10 μg/ml) caused NHKs to show minimal activation of Akt with strong activation of caspase 8, although HaCaT and A431 cells continued to show predomi-
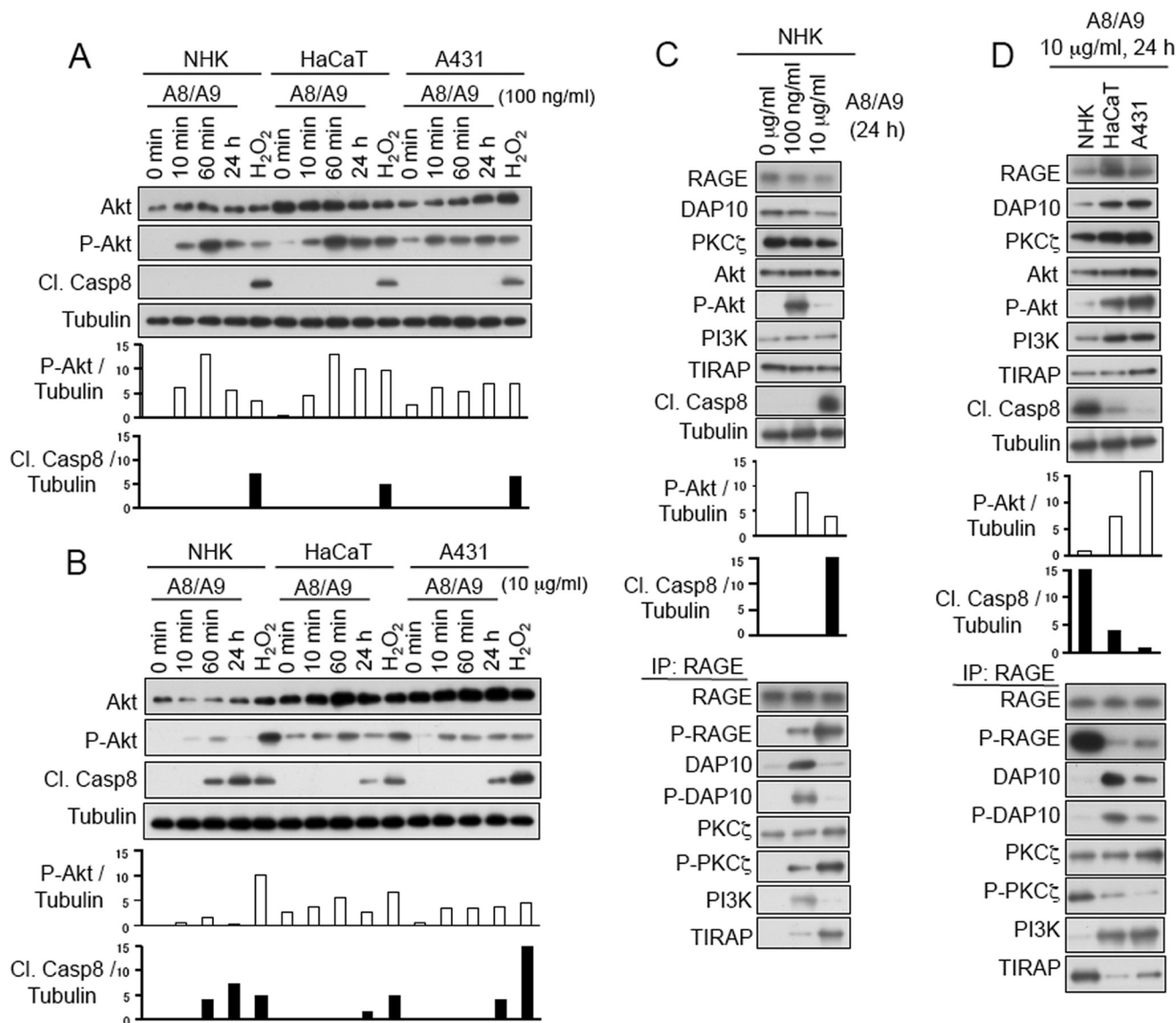
FIGURE 4. **S100A8/A9-triggered signaling is differentially regulated in NHKs, HaCaT cells, and A431 cells.** *A,* time-dependent activation of Akt and cleaved caspase 8 (*Cl. Casp8*) by S100A8/A9 at a low dose, 100 ng/ml, or (*B*) at a high dose, 10 μg/ml. H_2O_2 (500 μM, 3 h) was used as a positive control. *Bar graphs,* quantified levels of phosphorylated Akt and cleaved caspase 8 relative to tubulin. *C,* activation of adaptor and downstream signaling proteins by S100A8/A9. Twenty four hours after application of S100A8/A9 (0, 0.1, and 10 μg/ml), cell extracts were analyzed by Western blotting both with and without prior IP of endogenous RAGE using biotinylated anti-RAGE and streptavidin beads. *D,* activation of adaptor and downstream signaling proteins by a high concentration of S100A8/A9 (10 μg/ml) among different cell lines (NHKs, HaCaT cells, and A431 cells).

nant activation of Akt (Fig. 4*B*). With these results, we further extended our study to investigate possible signaling machinery(ies) that could have caused the cells to respond differently toward the treatment with S100A8/A9. Treatment with 100 ng/ml S100A8/A9 for 24 h in NHKs induced the strong activation of Akt, together with an increase in phosphorylation of DAP10 and recruitment of PI3K, whereas 10 μg/ml S100A8/A9 led to activation of caspase 8. This was followed by a higher phosphorylation level of PKCζ, its linked RAGE phosphorylation, and increased recruitment of TIRAP (Fig. 4*C*). Interestingly, exposure of 10 μg/ml S100A8/A9 in both HaCaT and A431 showed a RAGE-triggered signaling profile similar to that observed in NHKs exposed to 100 ng/ml but not 10 μg/ml S100A8/A9 (Fig. 4*D*). In accordance to these signal transduction profiles, 100 ng/ml S100A8/A9 stimulated the growth of

NHKs, but 10 μg/ml S100A8/A9 suppressed it. For HaCaT and A431 cells, even 10 μg/ml S100A8/A9 stimulated growth (Fig. 5*A*). In addition, we found that pharmacological inhibition of Akt signaling using an Akt inhibitor markedly abrogated growth enhancement in NHKs with low concentration of S100A8/A9 (100 ng/ml) and in HaCaT and A431 cells with both low (100 ng/ml) and high (10 μg/ml) concentrations of S100A8/A9 (Fig. 5*A*). Next, we found that high (10 μg/ml) concentration of S100A8/A9 actually induced apoptosis in NHKs but not in HaCaT and A431 cells. However, application of the Akt inhibitor resulted in induction of apoptosis by a high concentration of S100A8/A9 in HaCaT and A431 cells (Fig. 5*B*). Correspondingly, application of the Akt inhibitor caused activation of caspase 8 by a high concentration of S100A8/A9 in HaCaT and A431 cells, similar to that in NHKs without Akt
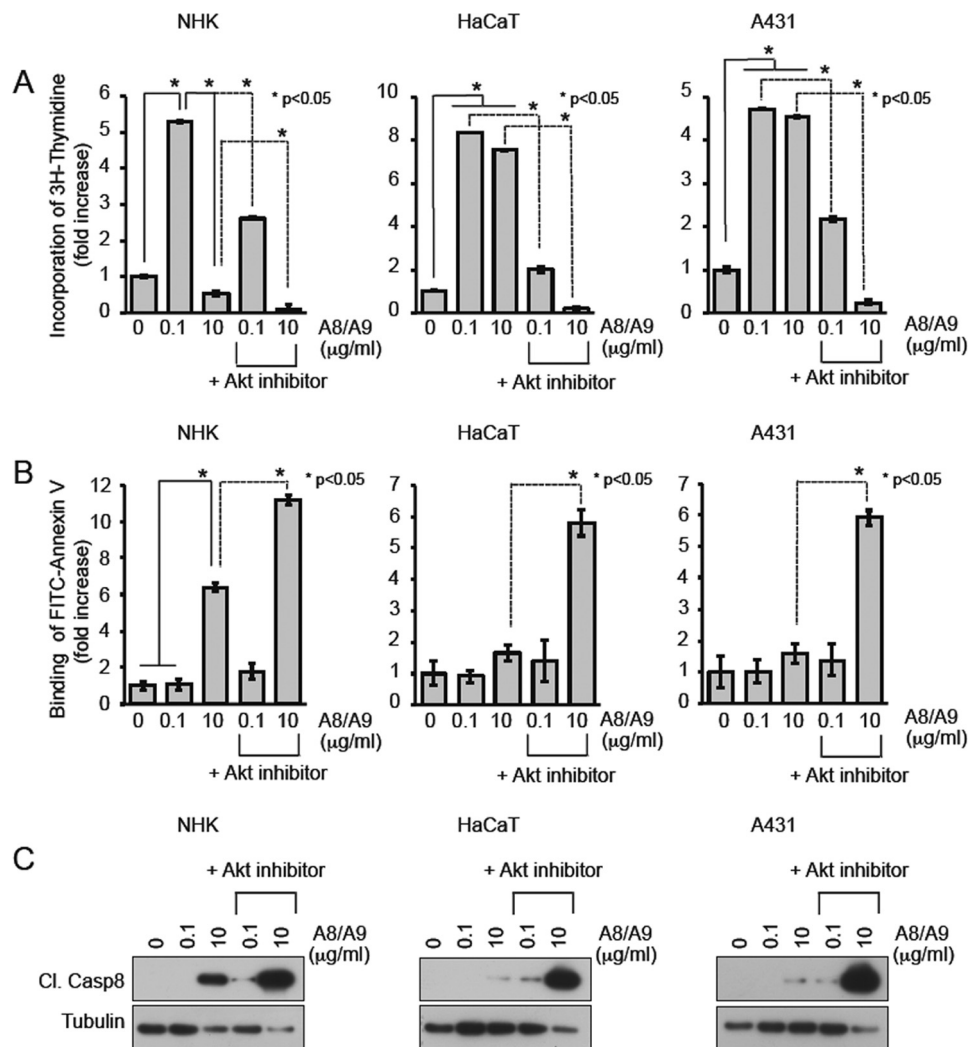
FIGURE 5. **Differential response to S100A8/A9 among NHKs, HaCaT cells, and A431 cells.** *A,* stimulation of DNA synthesis by S100A8/A9. The cells (NHKs (*left*), HaCaT cells (*middle*), and A431 cells (*right*)) were treated with S100A8/A9 (0, 0.1, and 10 μg/ml) for 24 h, and [^{3}H]thymidine (1 μCi/ml) was added to the cultures 1 h prior to harvesting of cells in the presence or absence of an Akt inhibitor (10 μM) (*, $p < 0.05$). *B,* induction of apoptosis by S100A8/A9 (24 h). FITC-labeled annexin V was added to the cultures 1 h prior to fluorescence counting of cells (*, $p < 0.05$). *C,* activation of cleaved caspase 8 (*Cl. Casp8*) by S100A8/A9 (24 h). The experiments shown in *B* and *C* were performed under conditions similar to those described in *A*.

inhibitor (Fig. 5C). Thus, Akt plays a critical role in S100A8/A9-mediated regulation of cellular proliferation and apoptosis.

To better understand the differential response of normal and transformed human keratinocytes to a high concentration of S100A8/A9 (10 μg/ml) in correlation with DAP10, the expression levels of endogenous DAP10 were examined. We found that endogenous DAP10 was remarkably overexpressed in HaCaT and A431 cells (Fig. 6A). This up-regulation of DAP10 was not affected by the presence or absence of nutritional supplements in the cultures (HKGS for NHKs; FBS for HaCaT and A431 cells). When DAP10 was down-regulated by siRNA, activation of Akt was abrogated, and caspase 8 was activated in both lines exposed to 10 μg/ml S100A8/A9. Phosphorylation of both RAGE and PKCζ was eventually up-regulated followed by recruitment of TIRAP and suppression of DAP10-PI3K binding (Fig. 6B). Moreover, down-regulation of DAP10 in HaCaT and A431 cells by siRNA in turn sensitized the cells to apoptosis by high concentrations of S100A8/A9 (Fig. 7A). However, the forced expression of a foreign DAP10 in NHKs resulted in a

higher resistance to apoptosis by a high concentration of S100A8/A9 (Fig. 7B). These observations in cell resistance and apoptosis patterns of DAP10 down-regulated HaCaT and A431 cells, and in DAP10 the up-regulated NHKs were similar to those seen in NHKs and in transformed cells, respectively, indicating that the differential response of normal and transformed human keratinocytes to different concentrations of S100A8/A9 is due to the extent of DAP10 involvement in RAGE signaling.

Overexpression of DAP10 in the Psoriatic Human Epidermis— To gain insight into the biological significance of the involvement of DAP10, we analyzed the normal human epidermis and psoriatic human epidermis by immunohistochemistry. In accordance with our previous report, S100A8/A9 was overexpressed in the lesional epidermis of patients with psoriasis vulgaris and pustular psoriasis (Fig. 8A). DAP10 was remarkably overexpressed in two different cases of psoriatic vulgaris and pustular psoriasis (Fig. 8B). A high level of phosphorylated Akt was also observed in the psoriatic epidermis. Finally, among the various growth factors and inflammatory cytokines applied in
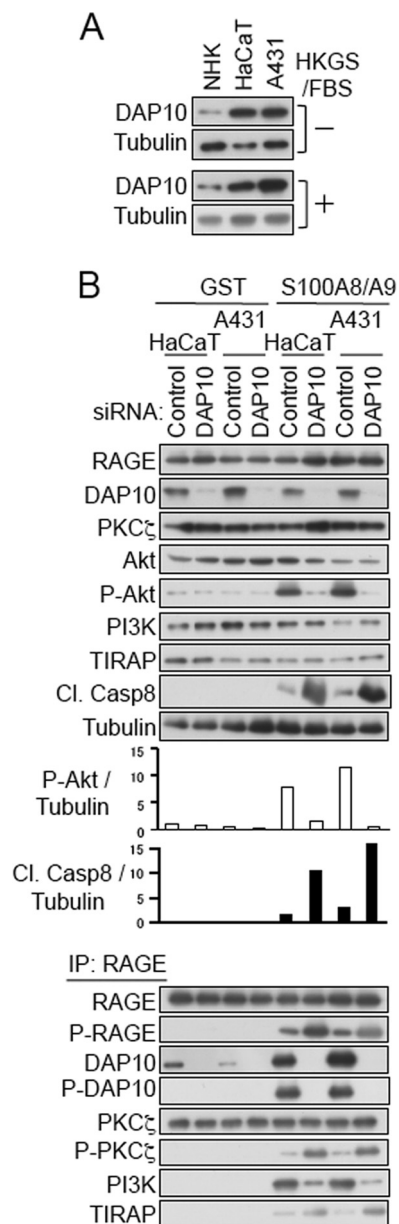
FIGURE 6. **Down-regulation of DAP10 modulates RAGE-triggered signaling.** *A,* increased expression of endogenous DAP10 in HaCaT and A431 cells compared with that in NHKs. The cells were cultured with or without supplements (HKGS for NHKs and FBS for HaCaT and A431 cells). Expression levels of endogenous DAP10 were determined by Western blot analysis. *B,* activation of adaptor and downstream signaling molecules upon down-regulation of DAP10 in HaCaT and A431 cells. Forty eight hours after transfection with 100 nM siRNAs, the cells were further incubated with GST or S100A8/A9 at 10 µg/ml for 24 h. Cell extracts were then prepared and analyzed by Western blotting with or without prior IP of endogenous RAGE using biotinylated anti-RAGE and streptavidin beads. *Bar graphs,* quantified levels of phosphorylated Akt and Cl. Casp8 relative to tubulin.

this study, only IL-22 remarkably induced DAP10 in NHKs (Fig. 9, *A* and *B*). Pretreatment with IL-22 protected NHKs against, to some degree, the apoptosis induced by a high concentration of S100A8/A9 (Fig. 9C), therefore indicating a certain level of involvement of IL-22 in the DAP10 overexpression.

DISCUSSION

In this study, we showed that DAP10 interacts with RAGE. DAP10 is known to be a transmembrane adaptor protein for the

NKG2D expressed in NK cells. Both DAP10 and NKG2D are also expressed on the surface of various types of cancer cells of epithelial origin (30). NKG2D recognizes nonclassical MHC class I antigens on the surface of cancer cells and transduces a signal via DAP10, leading to increased survival and proliferation (31). NKG2D and DAP10 interact through their transmembrane domain (26, 32). This method of interaction is shared not only by other known receptor proteins such as Sirp-b1 (33), Cd3001b (34), and Siglec-15 (35) but also by RAGE (Fig. 1D). Different from other receptor proteins where a negatively charged aspartic acid residue in the transmembrane region of DAP10 binds to a positively charged lysine, in RAGE, there is no positively charged residue in the transmembrane domain. At present, we cannot exclude the possibility that an unknown protein mediates the interaction between RAGE and DAP10. The use of a direct binding assay has been hampered by the extreme difficulty of purifying the two membrane proteins independently.

RAGE is known to transduce differential signals depending on the ligand concentration in certain biological contexts. For example, S100B promotes neurite outgrowth and protects neurons against oxidative stress at nanomolar levels, although it induces neuronal degeneration at micromolar levels (36). In another report, growth of NHKs was stimulated at nanomolar concentrations, but NHKs underwent apoptosis at micromolar concentrations of S100A8/A9 (Fig. 5) (18). These differential outcomes are at least partly due to the different intracellular signaling pathways downstream of RAGE (7, 8). In this study, we showed that DAP10 is involved in the selection of downstream signal transduction pathways. In an artificial multimerization system (Fig. 2, *A*–*C*), homomultimerization of RAGE led to activation of caspase 8, although heterodimerization of RAGE and DAP10 resulted in augmentation of growth/survival signals. In NHKs, S100A8/A9 appeared to induce heterodimerization of RAGE and DAP10 at lower concentrations but facilitated homomultimerization of RAGE at higher concentrations (Fig. 4C). However, transformed cells such as HaCaT and A431 cells, in which DAP10 was overexpressed (Fig. 6A), preferentially formed heterodimers even at a higher concentration of S100A8/A9 (Fig. 4D) because of the abundance of DAP10. Thus, DAP10 at least partly determines downstream signaling from ligand-activated RAGE.

In NHKs, DAP10 efficiently recruited PI3K upon binding to a low concentration (100 ng/ml) of S100A8/A9-stimulated RAGE and persistently activated Akt (Fig. 4C), leading to better survival (Fig. 5A). Persistent activation of Akt was also observed when NHKs were exposed to S100A11 (37). When DAP10 was down-regulated in NHKs, Akt was still activated but only transiently (Figs. 2E and 3, *A* and *B*), indicating that DAP10 is important for sustained Akt activation. It is known that a tyrosine residue (Tyr-86) in the YXXM motif of the intracellular domain of DAP10 recruits PI3K (p85) when phosphorylated (28). We confirmed that PI3K binds avidly to the RAGE-DAP10 complex (Figs. 1, *E* and *F*, and 2B). As we reported previously, RAGE has another adaptor protein pathway, *i.e.* TIRAP and MyD88 (21). Because MyD88 has the capacity to recruit PI3K (29), the observed transient activation of Akt in DAP10-de-
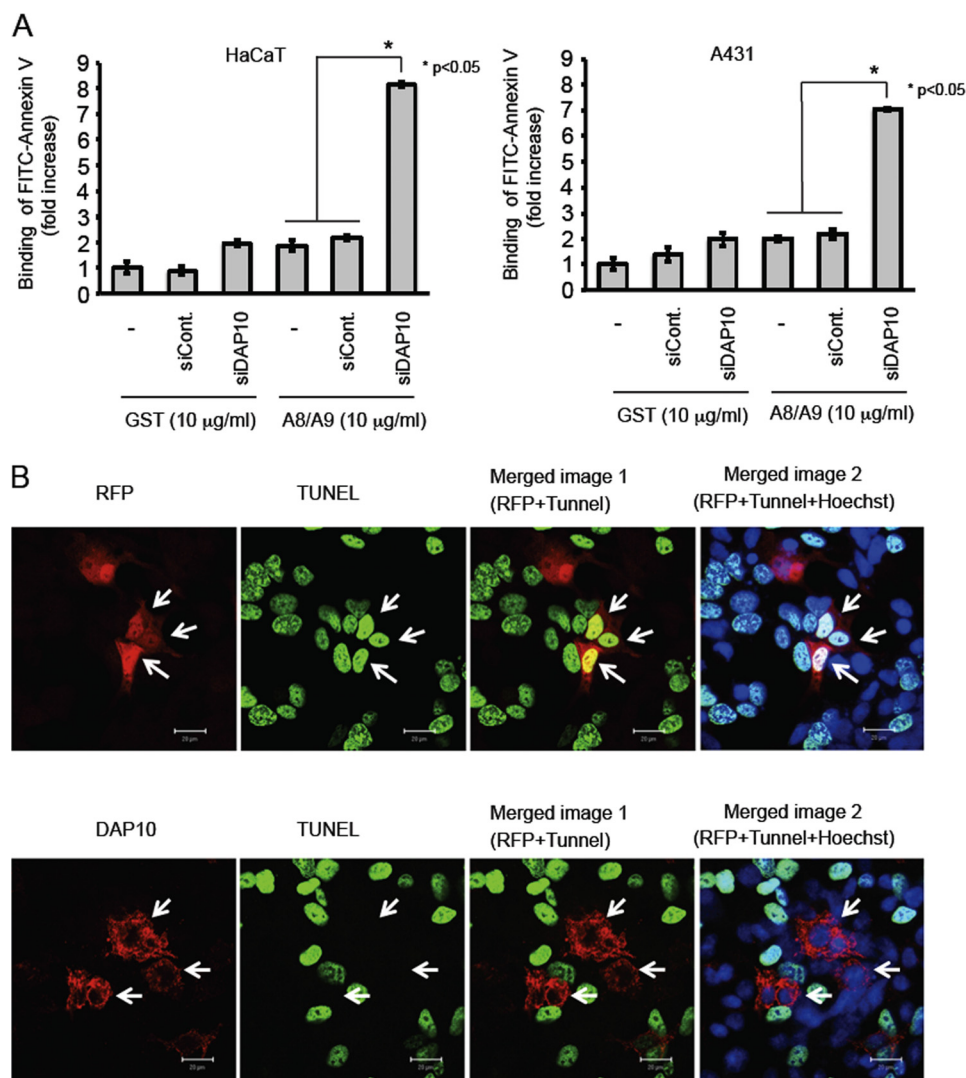
FIGURE 7. **DAP10-related cell survival.** *A*, sensitization of HaCaT and A431 cells to 10 μg/ml S100A8/A9-induced apoptosis by down-regulation of DAP10 (*, $p < 0.05$). The cells (HaCaT cells (*left*) and A431 cells (*right*)) were treated with siRNAs for 48 h, and apoptotic rates were determined using FITC-labeled annexin V. *B*, effects of forced expression of DAP10 on S100A8/A9-mediated apoptotic cell death. NHKs were transiently transfected with a plasmid expressing red fluorescence protein (*RFP*; negative control) or DAP10 tagged with C-terminal 3×FLAG-His[6]. After incubation for 48 h, the cells were treated with S100A8/A9 (10 μg/ml) for 24 h and then fixed with 4% paraformaldehyde. Sample slides were processed with a click-it TUNEL Alexa Fluor Imaging kit (Molecular Probes Invitrogen) for detecting apoptotic cells (*green*). The expression of DAP10 was visualized by indirect immunostaining with anti-FLAG antibody (*red*). Nuclei were stained with Hoechst 33342 (*blue*). *Scale bar*, 20 μm.

pleted cells likely occurred through this pathway (Figs. 2*E* and 3*B*).

As reported previously (21), PKCζ is essential for RAGE-triggered signal transduction. PKCζ is activated by autophosphorylation of Thr-560 at the C-terminal side (38). Homodimerization and homomultimerization of RAGE resulted in autophosphorylation of PKCζ (Thr-560) (Fig. 2*B*). Homodimerization and homomultimerization of RAGE probably led to mutual phosphorylation of associated PKCζ, and the activated PKCζ, in turn, phosphorylated Ser-391 of RAGE. The abundant DAP10 inhibited the homodimerization and homomultimerization and hence phosphorylation of Ser-391 of RAGE (Fig. 2*B*). Because phosphorylated Ser-391 is essential for the recruitment of TIRAP/MyD88 (21), the involvement of DAP10 in RAGE-triggered signaling leads to abrogation of caspase 8 activation and alternatively to sustained Akt activation (Fig. 2, *C* and *E*).

We do not think that the S100A8/A9-induced activation of Akt that is observed in various types of cells is solely mediated by RAGE-DAP10. Vogl *et al.* (39) reported that S100A8/A9 binds to TLR4, and we showed that Emmprin also functions as a receptor for S100A8/A9 (17). Akt is a downstream signal mediator for TLR4 and Emmprin (29, 40). In NHKs, the expression level of TLR4 was very low, but Emmprin was expressed at an appreciable level as assayed by quantitative RT-PCR (data not shown). In general, the expression profiles of RAGE, DAP10, TLR4, and Emmprin vary greatly depending on the cell type (data not shown). The partially overlapping functional interference among receptors and adaptor proteins, together with the variable expression profiles of the involved proteins, includes a complex signal processing unit.

IL-22 produced by skin-infiltrating lymphocytes is thought to be involved in the initiation and/or maintenance of psoriasis (41, 42). Application of IL-22 to an *in vitro* organotypic skin
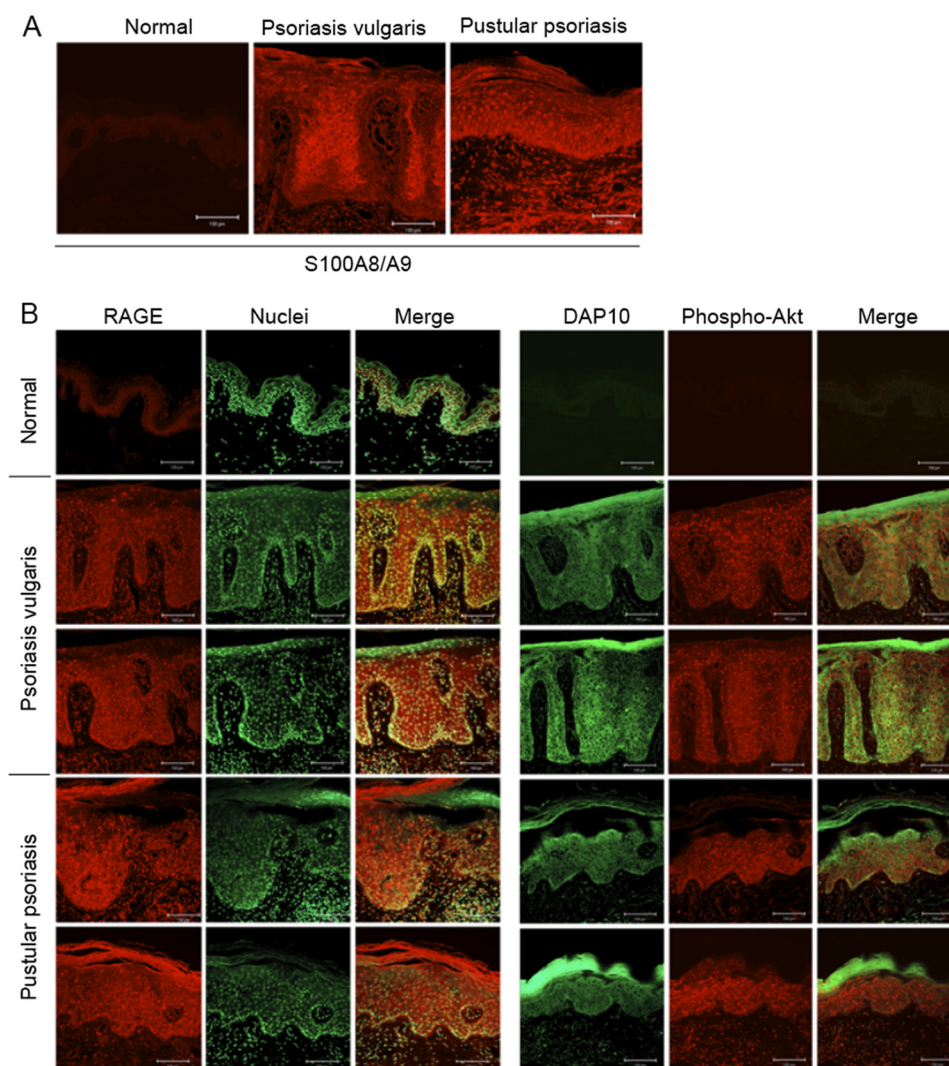
FIGURE 8. **Highly up-regulated expression of DAP10 in the epidermis of psoriatic lesions.** *A,* immunohistochemistry analysis for a RAGE ligand, S100A8/A9 heterodimer (*red*), in psoriatic lesions. S100A8/A9 was detected in keratinocytes and infiltrating inflammatory cells both in psoriasis vulgaris and pustular psoriasis. *B,* detection of RAGE (*red*), DAP10 (*green*), and phospho-Akt (*red*) in skin sections prepared from normal and psoriatic skin. Nuclei were stained with SYBR Green. *Bars* in *A* and *B*, 100 μm. *C,* induction of DAP10 by IL-22 applied to NHKs for 24 h.

model resulted in deterioration in terminal differentiation of the epidermis and hyperplastic epidermis with a reduced granular layer, which is often observed in psoriatic lesions (43, 44). Overexpression of IL-22 led to psoriasis-like hyperplasia in *in vivo* mouse skin (44). Injection of IL-23 into mouse skin also led to epidermal hyperplasia, which was abrogated in IL-22$^{-/-}$ mice and in mice treated with an antibody against IL-22 (45, 46). Van Belle *et al.* (47) showed that IL-22 is functionally involved in the pathogenesis of psoriasis with pustules induced by the TLR7/8 agonist imiquimod. As shown in Fig. 9, *A* and *B*, IL-22 induced a remarkable level of DAP10 in NHKs. It is well known that IL-22 is a potent inducer of S100A8/A9 (48, 49). Therefore, it is conceivable that an overexpression of S100A8/A9 and DAP10, induced at least in part by IL-22, plays a pivotal role in the pathogenesis of psoriasis.

Activated RAGE-DAP10 recruited not only PI3K but also GRB2 and GRB7 (Fig. 1, *E* and *F*). An interaction between GRB7 and DAP10 was newly found in this study. GRB2 and GRB7 are known to function as adaptor proteins for ErbB2 (50, 51) and lead to cellular proliferation via the activation of Ras (52, 53). It

is possible that GRB2 and GRB7 are involved in hyperproliferation of the epidermis in psoriatic lesions.

Accumulating evidence indicates that IL-22 is involved in cancer progression. IL-22 produced by infiltrating T cells and cancer cells themselves stimulates cell proliferation and enhances survival (54, 55). In addition, S100A8/A9, RAGE, and DAP10 are often overexpressed in various types of cancer (30, 56–59). The present findings regarding the functional interaction between RAGE and DAP10 may also be relevant to cancer progression.

Recently, IL-1R antagonists such as IL-1Ra and IL-36Ra have attracted attention due to their potential roles in the pathogenesis of pustular psoriasis (60). Mutation in IL-1Ra and deletion in IL-36Ra have been observed in patients with pustular psoriasis (61–64). A functional defect in the antagonists caused a failure in the control of inflammatory signals from the IL-1 receptor family. We previously reported that production of IL-1F9 (IL-36γ, an IL-36R agonist) was remarkably enhanced by S100A8/A9 in NHKs and that IL-1F9 in turn induced S100A8/A9 (positive feedback) (18). In IL-36Ra-deficient
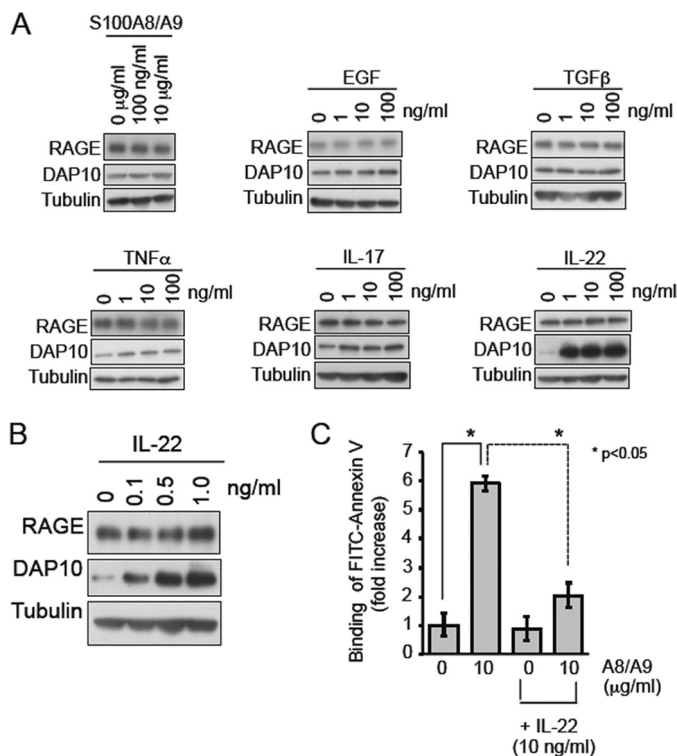
FIGURE 9. **Effects of IL-22 on S100A8/A9-mediated apoptotic cell death.** *A* and *B* expression levels of DAP10 and RAGE in NHKs. Twenty four hours after application of S100A8/A9, EGF, TGF-β, TNF-α, IL-17, and IL-22, the treated cell extracts were examined by Western blot analysis. *B*, effect of IL-22 at lower concentrations (0.1–1.0 ng/ml) on DAP10 expression in NHKs. *C*, protective effect of IL-22 on S100A8/A9-mediated apoptosis in NHKs. In the presence or absence of IL-22 (10 ng/ml), cells were treated with S100A8/A9 (10 μg/ml) for 24 h. FITC-labeled annexin V was added to the cultures 1 h prior to fluorescence counting of cells (*, $p < 0.05$).

patients, overproduction of S100A8/A9 may trigger an uncontrolled positive feedback mechanism for inflammation and hyperproliferation. In addition, we observed that activated RAGE leads to the induction of IL-1R agonists such as IL-1α and IL-1β (21).

In conclusion, we found that DAP10 is critically involved in RAGE-mediated survival signaling upon S100A8/A9 binding via the sustained activation of Akt. Both the concentrations of ligands and the expression levels of DAP10 affected the signaling pathways downstream from RAGE, but in a different manner. Such differential signaling has been observed in psoriatic epidermal cells and cancer cells but not in their normal counterparts, and thus has been implicated in the pathogenesis of these conditions. We hope that our findings will lead to a better understanding of the physiological and pathological conditions of keratinocytes and the development of therapeutic measures against various skin diseases.

REFERENCES

1. Ramasamy, R., Yan, S. F., and Schmidt, A. M. (2009) RAGE: therapeutic target and biomarker of the inflammatory response—the evidence mounts. *J. Leukocyte Biol.* **86,** 505–512
2. Sims, G. P., Rowe, D. C., Rietdijk, S. T., Herbst, R., and Coyle, A. J. (2010) HMGB1 and RAGE in inflammation and cancer. *Annu. Rev. Immunol.* **28,** 367–388
3. Yan, S. F., Ramasamy, R., and Schmidt, A. M. (2010) Soluble RAGE: therapy and biomarker in unraveling the RAGE axis in chronic disease and aging. *Biochim. Pharmacol.* **79,** 1379–1386
4. Yan, S. F., Ramasamy, R., and Schmidt, A. M. (2010b) The RAGE axis: a fundamental mechanism signaling danger to the vulnerable vasculature. *Circ. Res.* **106,** 842–853
5. Gebhardt, C., Riehl, A., Durchdewald, M., Németh, J., Fürstenberger, G., Müller-Decker, K., Enk, A., Arnold, B., Bierhaus, A., Nawroth, P. P., Hess, J., and Angel, P. (2008) RAGE signaling sustains inflammation and promotes tumor development. *J. Exp. Med.* **205,** 275–285
6. González, I., Romero, J., Rodríguez, B. L., Pérez-Castro, R., and Rojas, A. (2013) The immunobiology of the receptor of advanced glycation end-products: Trends and challenges. *Immunobiology* **218,** 790–797
7. Kierdorf, K., and Fritz, G. (2013) RAGE regulation and signaling in inflammation and beyond. *J. Leukocyte Biol.* **94,** 55–68
8. Sorci, G., Riuzzi, F., Giambanco, I., and Donato, R. (2013) RAGE in tissue homeostasis, repair and regeneration. *Biochim. Biophys. Acta* **1833,** 101–109
9. Pricci, F., Leto, G., Amadio, L., Iacobini, C., Romeo, G., Cordone, S., Gradini, R., Barsotti, P., Liu, F. T., Di Mario, U., and Pugliese, G. (2000) Role of galectin-3 as a receptor for advanced glycosylation end products. *Kidney Int. Suppl.* **77,** S31–S39
10. Ohgami, N., Nagai, R., Ikemoto, M., Arai, H., Kuniyasu, A., Horiuchi, S., and Nakayama, H. (2001) Cd36, a member of the class B scavenger receptor family, as a receptor for advanced glycation end products. *J. Biol. Chem.* **276,** 3195–3202
11. Ohgami, N., Nagai, R., Miyazaki, A., Ikemoto, M., Arai, H., Horiuchi, S., and Nakayama, H. (2001) Scavenger receptor class B type I-mediated reverse cholesterol transport is inhibited by advanced glycation end products. *J. Biol. Chem.* **276,** 13348–13355
12. Jono, T., Miyazaki, A., Nagai, R., Sawamura, T., Kitamura, T., and Horiuchi, S. (2002) Lectin-like oxidized low density lipoprotein receptor-1 (LOX-1) serves as an endothelial receptor for advanced glycation end products (AGE). *FEBS Lett.* **511,** 170–174
13. Tamura, Y., Adachi, H., Osuga, J., Ohashi, K., Yahagi, N., Sekiya, M., Okazaki, H., Tomita, S., Iizuka, Y., Shimano, H., Nagai, R., Kimura, S., Tsujimoto, M., and Ishibashi, S. (2003) FEEL-1 and FEEL-2 are endocytic receptors for advanced glycation end products. *J. Biol. Chem.* **278,** 12613–12617
14. Horiuchi, S., Unno, Y., Usui, H., Shikata, K., Takaki, K., Koito, W., Sakamoto, Y., Nagai, R., Makino, K., Sasao, A., Wada, J., and Makino, H. (2005) Pathological roles of advanced glycation end product receptors SR-A and CD36. *Ann. N.Y. Acad. Sci.* **1043,** 671–675
15. Tang, S. C., Lathia, J. D., Selvaraj, P. K., Jo, D. G., Mughal, M. R., Cheng, A., Siler, D. A., Markesbery, W. R., Arumugam, T. V., and Mattson, M. P. (2008) Toll-like receptor-4 mediates neuronal apoptosis induced by amyloid β-peptide and the membrane lipid peroxidation product 4-hydroxynonenal. *Exp. Neurol.* **213,** 114–121
16. van Beijnum, J. R., Buurman, W. A., and Griffioen, A. W. (2008) Convergence and amplification of toll-like receptor (TLR) and receptor for advanced glycation end products (RAGE) signaling pathways via high mobility group B1 (HMGB1). *Angiogenesis* **11,** 91–99
17. Hibino, T., Sakaguchi, M., Miyamoto, S., Yamamoto, M., Motoyama, A., Hosoi, J., Shimokata, T., Ito, T., Tsuboi, R., and Huh, N. H. (2013) S100A9 is a novel ligand of EMMPRIN that promotes melanoma metastasis. *Cancer Res.* **73,** 172–183
18. Nukui, T., Ehama, R., Sakaguchi, M., Sonegawa, H., Katagiri, C., Hibino, T., and Huh, N. H. (2008) S100A8/A9, a key mediator for positive feedback growth stimulation of normal human keratinocytes. *J. Cell. Biochem.* **104,** 453–464
19. Zenz, R., Eferl, R., Kenner, L., Florin, L., Hummerich, L., Mehic, D., Scheuch, H., Angel, P., Tschachler, E., and Wagner, E. F. (2005) Psoriasis-like skin disease and arthritis caused by inducible epidermal deletion of Jun proteins. *Nature* **437,** 369–375
20. Aochi, S., Tsuji, K., Sakaguchi, M., Huh, N., Tsuda, T., Yamanishi, K., Komine, M., and Iwatsuki, K. (2011) Markedly elevated serum levels of calcium-binding S100A8/A9 proteins in psoriatic arthritis are due to activated monocytes/macrophages. *J. Am. Acad. Dermatol.* **64,** 879–887
21. Sakaguchi, M., Murata, H., Yamamoto, K., Ono, T., Sakaguchi, Y., Motoyama, A., Hibino, T., Kataoka, K., and Huh, N. H. (2011) TIRAP, an adaptor protein for TLR2/4, transduces a signal from RAGE phosphory-

lated upon ligand binding. *PLoS One* **6,** e23132

22. Hudson, B. I., Kalea, A. Z., Del Mar Arriero, M., Harja, E., Boulanger, E., D'Agati, V., and Schmidt, A. M. (2008) Interaction of the RAGE cytoplasmic domain with diaphanous-1 is required for ligand-stimulated cellular migration through activation of Rac1 and Cdc42. *J. Biol. Chem.* **283,** 34457–34468

23. Gay, N. J., and Gangloff, M. (2007) Structure and function of Toll receptors and their ligands. *Annu. Rev. Biochem.* **76,** 141–165

24. Zong, H., Madden, A., Ward, M., Mooney, M. H., Elliott, C. T., and Stitt, A. W. (2010) Homodimerization is essential for the receptor for advanced glycation end products (RAGE)-mediated signal transduction. *J. Biol. Chem.* **285,** 23137–23146

25. Slowik, A., Merres, J., Elfgen, A., Jansen, S., Mohr, F., Wruck, C. J., Pufe, T., and Brandenburg, L. O. (2012) Involvement of formyl peptide receptors in receptor for advanced glycation end products (RAGE) -and amyloid β 1–42-induced signal transduction in glial cells. *Mol. Neurodegener.* **7,** 55

26. Lanier, L. L. (2009) DAP10- and DAP12-associated receptors in innate immunity. *Immunol. Rev.* **227,** 150–160

27. Upshaw, J. L., Arneson, L. N., Schoon, R. A., Dick, C. J., Billadeau, D. D., and Leibson, P. J. (2006) NKG2D-mediated signaling requires a DAP10-bound Grb2-Vav1 intermediate and phosphatidylinositol-3-kinase in human natural killer cells. *Nat. Immunol.* **7,** 524–532

28. Lanier, L. L. (2008) Up on the tightrope: natural killer cell activation and inhibition. *Nat. Immunol.* **9,** 495–502

29. Laird, M. H., Rhee, S. H., Perkins, D. J., Medvedev, A. E., Piao, W., Fenton, M. J., and Vogel, S. N. (2009) TLR4/MyD88/PI3K interactions regulate TLR4 signaling. *J. Leukocyte Biol.* **85,** 966–977

30. Benitez, A. C., Dai, Z., Mann, H. H., Reeves, R. S., Margineantu, D. H., Gooley, T. A., Groh, V., and Spies, T. (2011) Expression, signaling proficiency, and stimulatory function of the NKG2D lymphocyte receptor in human cancer cells. *Proc. Natl. Acad. Sci. U.S.A.* **108,** 4081–4086

31. Obeidy, P., and Sharland, A. F. (2009) NKG2D and its ligands. *Int. J. Biochem. Cell Biol.* **41,** 2364–2367

32. Wu, J., Song, Y., Bakker, A. B., Bauer, S., Spies, T., Lanier, L. L., and Phillips, J. H. (1999) An activating immunoreceptor complex formed by NKG2D and DAP10. *Science* **285,** 730–732

33. Anfossi, N., Lucas, M., Diefenbach, A., Bühring, H. J., Raulet, D., Tomasello, A., and Vivier, E. (2003) Contrasting roles of DAP10 and KARAP/DAP12 signaling adaptors in activation of the RBL-2H3 leukemic mast cell line. *Eur. J. Immunol.* **33,** 3514–3522

34. Yamanishi, Y., Kitaura, J., Izawa, K., Matsuoka, T., Oki, T., Lu, Y., Shibata, F., Yamazaki, S., Kumagai, H., Nakajima, H., Maeda-Yamamoto, M., Tybulewicz, V. L., Takai, T., and Kitamura, T. (2008) Analysis of mouse LMIR5/CLM-7 as an activating receptor: differential regulation of LMIR5/CLM-7 in mouse *versus* human cells. *Blood* **111,** 688–698

35. Angata, T., Tabuchi, Y., Nakamura, K., and Nakamura, M. (2007) Siglec-15: an immune system Siglec conserved throughout vertebrate evolution. *Glycobiology* **17,** 838–846

36. Huttunen, H. J., Kuja-Panula, J., Sorci, G., Agnelleti, A. L., Donato, R., and Rauvala, H. (2000) Coregulation of neurite outgrowth and cell survival by amphoterin and S100 proteins through receptor for advanced glycation end products (RAGE) activation. *J. Biol. Chem.* **275,** 40096–40105

37. Sakaguchi, M., Sonegawa, H., Murata, H., Kitazoe, M., Futami, J., Kataoka, K., Yamada, H., and Huh, N. H. (2008) S100A11, an dual mediator for growth regulation of human keratinocytes. *Mol. Biol. Cell* **19,** 78–85

38. Hirai, T., and Chida, K. (2003) Protein kinase czeta (PKCzeta): Activation mechanisms and cellular functions. *J. Biochem.* **133,** 1–7

39. Vogl, T., Tenbrock, K., Ludwig, S., Leukert, N., Ehrhardt, C., van Zoelen, M. A., Nacken, W., Foell, D., van der Poll, T., Sorg, C., and Roth, J. (2007) Mrp8 and Mrp14 are endogenous activators of Toll-like receptor 4, promoting lethal, endotoxin-induced shock. *Nat. Med.* **13,** 1042–1049

40. Tang, Y., Nakada, M. T., Rafferty, P., Laraio, J., McCabe, F. L., Millar, H., Cunningham, M., Snyder, L. A., Bugelski, P., and Yan, L. (2006) Regulation of vascular endothelial growth factor expression by EMMPRIN via the PI3K-Akt signaling pathway. *Mol. Cancer Res.* **4,** 371–377

41. Boniface, K., Guignouard, E., Pedretti, N., Garcia, M., Delwail, A., Bernard, F. X., Nau, F., Guillet, G., Dagregorio, G., Yssel, H., Lecron, J. C., and Morel, F. (2007) A role for T cell-derived interleukin 22 in psoriatic skin

42. Zhang, N., Pan, H. F., and Ye, D. Q. (2011) Th22 in inflammatory and autoimmune disease: prospects for therapeutic intervention. *Mol. Cell. Biochem.* **353,** 41–46

43. Nograles, K. E., Zaba, L. C., Guttman-Yassky, E., Fuentes-Duculan, J., Suárez-Fariñas, M., Cardinale, I., Khatcherian, A., Gonzalez, J., Pierson, K. C., White, T. R., Pensabene, C., Coats, I., Novitskaya, I., Lowes, M. A., and Krueger, J. G. (2008) Th17 cytokines interleukin (IL)-17 and IL-22 modulate distinct inflammatory and keratinocyte-response pathways. *Br. J. Dermatol.* **159,** 1092–1102

44. Wolk, K., Haugen, H. S., Xu, W., Witte, E., Waggie, K., Anderson, M., Vom Baur, E., Witte, K., Warszawska, K., Philipp, S., Johnson-Leger, C., Volk, H. D., Sterry, W., and Sabat, R. (2009) IL-22 and IL-20 are key mediators of the epidermal alterations in psoriasis while IL-17 and IFN-γ are not. *J. Mol. Med.* **87,** 523–536

45. Zheng, Y., Danilenko, D. M., Valdez, P., Kasman, I., Eastham-Anderson, J., Wu, J., and Ouyang, W. (2007) Interleukin-22, a T(H)17 cytokine, mediates IL-23-induced dermal inflammation and acanthosis. *Nature* **445,** 648–651

46. Rizzo, H. L., Kagami, S., Phillips, K. G., Kurtz, S. E., Jacques, S. L., and Blauvelt, A. (2011) IL-23-mediated psoriasis-like epidermal hyperplasia is dependent on IL-17A. *J. Immunol.* **186,** 1495–1502

47. Van Belle, A. B., de Heusch, M., Lemaire, M. M., Hendrickx, E., Warnier, G., Dunussi-Joannopoulos, K., Fouser, L. A., Renauld, J. C., and Dumoutier, L. (2012) IL-22 is required for imiquimod-induced psoriasiform skin inflammation in mice. *J. Immunol.* **188,** 462–469

48. Wolk, K., Witte, E., Wallace, E., Döcke, W. D., Kunz, S., Asadullah, K., Volk, H. D., Sterry, W., and Sabat, R. (2006) IL-22 regulates the expression of genes responsible for antimicrobial defense, cellular differentiation, and mobility in keratinocytes: a potential role in psoriasis. *Eur. J. Immunol.* **36,** 1309–1323

49. Sonnenberg, G. F., Fouser, L. A., and Artis, D. (2011) Border patrol: regulation of immunity, inflammation and tissue homeostasis at barrier surfaces by IL-22. *Nat. Immunol.* **12,** 383–390

50. Stein, D., Wu, J., Fuqua, S. A., Roonprapunt, C., Yajnik, V., D'Eustachio, P., Moskow, J. J., Buchberg, A. M., Osborne, C. K., and Margolis, B. (1994) The SH2 domain protein GRB-7 is co-amplified, overexpressed and in a tight complex with HER2 in breast cancer. *EMBO J.* **13,** 1331–1340

51. Pradip, D., Bouzyk, M., Dey, N., and Leyland-Jones, B. (2013) Dissecting GRB7-mediated signals for proliferation and migration in HER2 overexpressing breast tumor cells: GTPase rules. *Am J. Cancer Res.* **3,** 173–195

52. Gale, N. W., Kaplan, S., Lowenstein, E. J., Schlessinger, J., and Bar-Sagi, D. (1993) Grb2 mediates the EGF-dependent activation of guanine nucleotide exchange on Ras. *Nature* **363,** 88–92

53. Chu, P. Y., Li, T. K., Ding, S. T., Lai, I. R., and Shen, T. L. (2010) EGF-induced Grb7 recruits and promotes Ras activity essential for the tumorigenicity of Sk-Br3 breast cancer cells. *J. Biol. Chem.* **285,** 29279–29285

54. Zhuang, Y., Peng, L. S., Zhao, Y. L., Shi, Y., Mao, X. H., Guo, G., Chen, W., Liu, X. F., Zhang, J. Y., Liu, T., Luo, P., Yu, P. W., and Zou, Q. M. (2012) Increased intratumoral IL-22-producing CD4(+) T cells and Th22 cells correlate with gastric cancer progression and predict poor patient survival. *Cancer Immunol. Immunother.* **61,** 1965–1975

55. Zhang, W., Chen, Y., Wei, H., Zheng, C., Sun, R., Zhang, J., and Tian, Z. (2008) Antiapoptotic activity of autocrine interleukin-22 and therapeutic effects of interleukin-22-small interfering RNA on human lung cancer xenografts. *Clin. Cancer Res.* **14,** 6432–6439

56. Hermani, A., Hess, J., De Servi, B., Medunjanin, S., Grobholz, R., Trojan, L., Angel, P., and Mayer, D. (2005) Calcium-binding proteins S100A8 and S100A9 as novel diagnostic markers in human prostate cancer. *Clin. Cancer Res.* **11,** 5146–5152

57. Gebhardt, C., Németh, J., Angel, P., and Hess, J. (2006) S100A8 and S100A9 in inflammation and cancer. *Biochem. Pharmacol.* **72,** 1622–1631

58. Kostova, N., Zlateva, S., Ugrinova, I., and Pasheva, E. (2010) The expression of HMGB1 protein and its receptor RAGE in human malignant tumors. *Mol. Cell. Biochem.* **337,** 251–258

59. Kang, R., Loux, T., Tang, D., Schapiro, N. E., Vernon, P., Livesey, K. M., Krasinskas, A., Lotze, M. T., and Zeh, H. J., 3rd (2012) The expression of the receptor for advanced glycation endproducts (RAGE) is permis-

sive for early pancreatic neoplasia. *Proc. Natl. Acad. Sci. U.S.A.* **109,** 7031–7036

60. Cowen, E. W., and Goldbach-Mansky, R. (2012) DIRA, DITRA, and new insights into pathways of skin inflammation: what's in a name? *Arch. Dermatol.* **148,** 381–384

61. Shepherd, J., Little, M. C., and Nicklin, M. J. (2004) Psoriasis-like cutaneous inflammation in mice lacking interleukin-1 receptor antagonist. *J. Invest. Dermatol.* **122,** 665–669

62. Jesus, A. A., Osman, M., Silva, C. A., Kim, P. W., Pham, T. H., Gadina, M., Yang, B., Bertola, D. R., Carneiro-Sampaio, M., Ferguson, P. J., Renshaw, B. R., Schooley, K., Brown, M., Al-Dosari, A., Al-Alami, J., Sims, J. E., Goldbach-Mansky, R., and El-Shanti, H. (2011) A novel mutation of IL1RN in the deficiency of interleukin-1 receptor antagonist syndrome:

description of two unrelated cases from Brazil. *Arthritis Rheum.* **63,** 4007–4017

63. Minkis, K., Aksentijevich, I., Goldbach-Mansky, R., Magro, C., Scott, R., Davis, J. G., Sardana, N., and Herzog, R. (2012) Interleukin 1 receptor antagonist deficiency presenting as infantile pustulosis mimicking infantile pustular psoriasis. *Arch. Dermatol.* **148,** 747–752

64. Marrakchi, S., Guigue, P., Renshaw, B. R., Puel, A., Pei, X. Y., Fraitag, S., Zribi, J., Bal, E., Cluzeau, C., Chrabieh, M., Towne, J. E., Douangpanya, J., Pons, C., Mansour, S., Serre, V., Makni, H., Mahfoudh, N., Fakhfakh, F., Bodemer, C., Feingold, J., Hadj-Rabia, S., Favre, M., Genin, E., Sahbatou, M., Munnich, A., Casanova, J. L., Sims, J. E., Turki, H., Bachelez, H., and Smahi, A. (2011) Interleukin-36-receptor antagonist deficiency and generalized pustular psoriasis. *N. Engl. J. Med.* **365,** 620–628